Extended Abstracts of the 2013 International Conference on Solid State Devices and Materials, Fukuoka, 2013, pp824-825

Experimental Study on Micro Optical Diffusion Sensor for Dynamic Sensing of Conformation Change

Yasunari Kadota[1], Yoshiaki Matoba[1], Yohei Ishii[1], Yoshihiro Taguchi[1], and Yuji Nagasaka[1]

[1] Keio Univ.
Department of System Design Engineering,
3-14-1 Hiyoshi, Yokohama, 223-8522, JAPAN
Phone: +81-45-566-1809 E-mail: tag@sd.keio.ac.jp

Abstract

We have newly developed a micro optical diffusion sensor, enabling high-speed, non-contact, and small sample volume sensing of biological sample. In this paper, the validity of the measurement principle is experimentally confirmed, and the novel scanning mirror for the POCT is proposed.

1. Introduction

The diffusion coefficient is important parameter for the analysis of the conformation changes of the biological sample including protein. From the viewpoint of Point of Care Testing and massively parallel processing in the field of drug discovery, a miniaturized one-chip sensing device that can achieve a high-speed and high-throughput measurement of the diffusion coefficient is required. However conventional methods (e.g. fluorescence correlation spectroscopy and nuclear magnetic resonance method) need bulk sample volume, and take a long time. Furthermore, they are difficult to miniaturize. From above aspects, we have developed a novel micro optical diffusion sensor (MODS) [1] based on laser-induced dielectrophoresis (LIDEP) [2], enabling minutely small sample and high-speed measurement without sample pretreatment. In this paper, in order to observe the mass diffusion generated by LIDEP, we propose a novel optical signal detection technique using diffracted light and a novel scanning mirror, which can be easily integrated into MODS. Then, we confirmed the validity of the proposed micro devices.

2. Measurement Principle

A schematic image of MODS is shown in Fig. 1. MODS consists of upper dielectrophoretic cell, namely DEP cell, and lower micro Fresnel mirror device. The micro Fresnel mirror [3] excites the interference pattern, and then the concentration distribution is generated by dielectrophoresis in DEP cell. In our final goal, all optical components and detection apparatuses are integrated into chip. The cross-sectional view of the DEP cell is shown in Fig. 2. The DEP cell consists of two transparent electrodes and photoconductive layer. Liquid sample is sealed within the micro channel. First, two excitation lasers are intersected on the photoconductive layer, and the sinusoidal light intensity distribution generates the sinusoidal distribution of electrical conductivity by the photoconductive effect. A non-uniform electric field is formed in the channel followed by generating the dielectrophoresis, and then the sinusoidal concentration distribution is induced. The concentration distribution is considered as diffraction grating, therefore the diffracted light is generated by irradiating probing laser. The decay of the concentration distribution occurs immediately after stopping the AC voltage, due to the mass diffusion of the particles. Diffusion coefficient can be measured by detecting the intensity decay of the diffracted light, and calculated according to the following equation.

$$D = \frac{1}{\tau_D}\left(\frac{\Lambda}{2\pi}\right)^2$$

D: Diffusion coefficient [m^2/s], τ_D: Decay time constant [s], Λ: The length of interference fringe spaces [m]

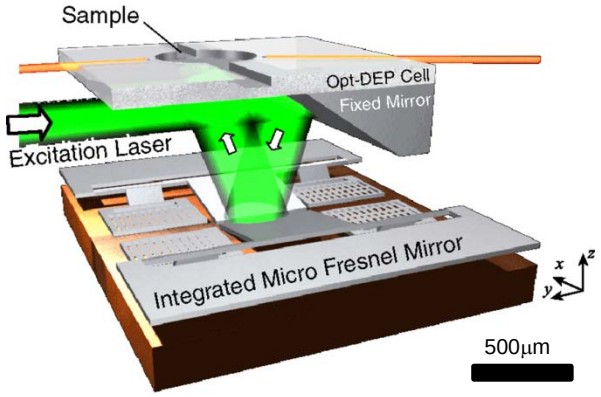

Fig.1 Schematic image of MODS.

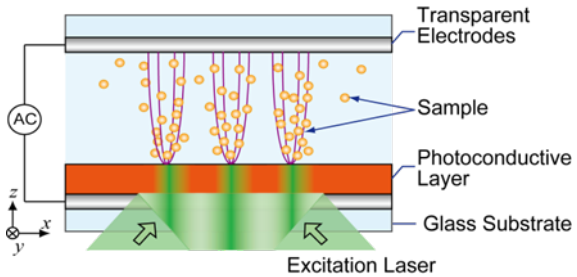

Fig.2 Generation of sinusoidal concentration distribution.

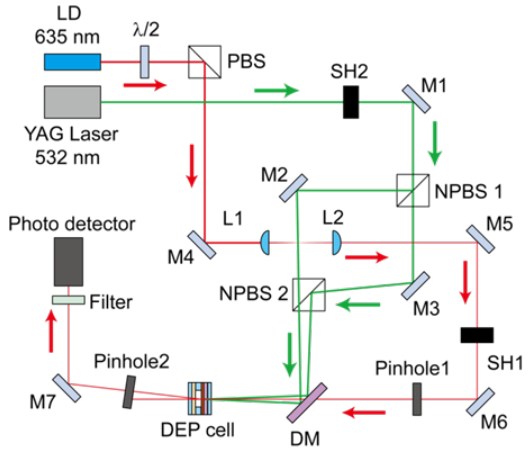

Fig.3 Schematic diagram of bench-top apparatus of MODS.

Table I Measurement Conditions

Channel Thickness	40 μm
Fringe Space Λ	10.5 μm
Visibility	0.96
Probing Light Intensity	5.9 mW
Excitation Light Intensity	3.2 mW
Excitation Time	5 s
Applied Voltage	10 $V_{p\text{-}p}$
Frequency	10 kHz

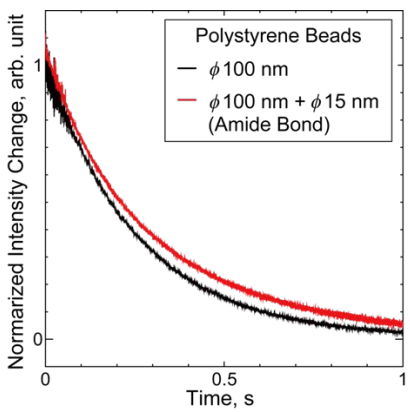

Fig.4 Signal change due to the Amide-bonding.

3. Experimental results using bench-top apparatus

In order to confirm the applicability of proposed method for the dynamic sensing of conformation change of bio-material, the dynamic change of diffusion coefficient depending on the size of the sample was observed by using the bench-top apparatus as shown in Fig. 3. YAG laser is divided into two beams by the beam splitter, and two beams are intersected on the DEP cell. The mass diffusion process of the sinusoidal concentration distribution generated by the DEP force is observed by the first-order diffracted beam of the probing laser. The experimental conditions are summarized in Table I. The signal change of the mass diffusion due to the modification of 15 nm-polystyrene beads on the 100nm-beads was successfully observed in Fig. 4. Therefore, the validity of our method was experimentally confirmed.

4. FEM analysis of comb-driven MFM

The comb-driven MFM is required in order to control the fringe space of the interference pattern, which is enabling the optimization of the measurement condition during the conformation change of the sample. Fig. 5 shows the fabrication process of comb-driven MFM, and the FEM simulation result is shown in Fig. 6. The slanted angle of MFM can be controlled by changing the applied voltage, and the applicability of proposed device was confirmed.

3. Conclusions

We have experimentally and analytically confirmed the validity of proposed micro optical diffusion sensor with comb-driven MFM for the POCT application.

Acknowledgements

This research was partially supported by the Japan Society for the Promotion of Science (JSPS), a Grant-in-Aid for Scientific Research (S, No.24226006), and a Ministry of Education, Culture, Sports, Science and Technology (MEXT) Grant-in-Aid for young Scientists (A, No.23686036). A part of this research was conducted at the KEIO satellite-center of "Low-Carbon Research Network" funded by the Ministry of Education, Culture, Sports, Science and Technology (MEXT), Japan.

References

[1] K. Itani *et al.*, *Netsu Bussei*, **23** 4(2009) 197.
[2] A.T. Ohta, *IEEE Journal of Selected Topics in Quantum Electronics*, **13** 2 (2007) 235.
[3] T. Oka *et al.*, *J. MEMS* **21** 2(2012) 324.

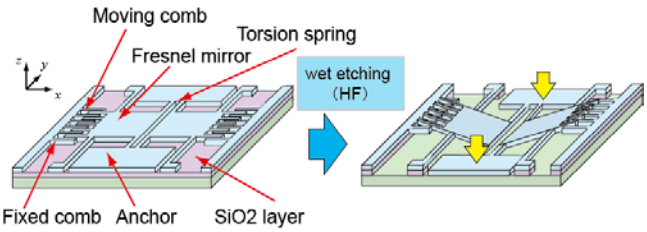

Fig. 5 Fabrication process of comb-driven MFM.

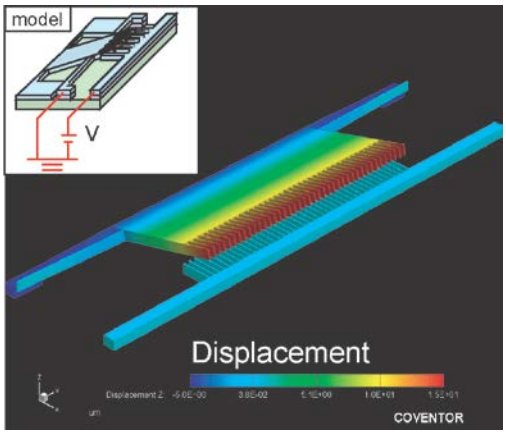

Fig.6 FEM simulation of comb-driven MFM.